Receding Horizon control of a compliant manipulator: experimental analysis

P. Boscariol*
DIEGM
University of Udine
Udine, Italy

A. Gasparetto
DIEGM
University of Udine
Udine, Italy

M. Giovagnoni
DIEGM
University of Udine
Udine, Italy

A. Lanzutti
DIEGM
University of Udine
Udine, Italy

R. Vidoni
DIEGM
University of Udine
Udine, Italy

V. Zanotto
DIEGM
University of Udine
Udine, Italy

Abstract—*This paper presents an experimental study of a Model Predictive Control scheme (MPC) for active vibration damping in flexible-link robotic manipulators (FLM). The prediction capability of the controller is based on a very accurate FEM dynamic model of planar FLMs. Experiments are performed on a laboratory prototype of a single-link mechanism affected by gravity force. Results show that the proposed controller achieves a good position tracking performance and an effective vibration suppression for wide range movements. Good performance are confirmed trough the comparison with a classical controller.*

Keywords: flexible-link robot, mechanical vibration, FLM

I. Introduction

Dynamics and control of flexible-link mechanisms are topics of a widespread interest in the scientific literature. From the 70's, a large number of papers have been published: Dwivedy [1] cites 433 works from 1975 to 2005 on the modeling of this class of mechanism and Benosman [2] cites 119 papers up to 2003. This popularity is motivated by several advantages of flexible-link manipulators over their rigid counterpart, such as lower weight, higher operative speed and reduced power consumption. Nevertheless, specific solutions in terms of control must be used to reach satisfactory performance, high accuracy and stability.

Over the years different control strategies have been proposed, such as robust control [3], [4], event-based control [5], vision-based control [6], just to name some of the most recent contributions. Most of the control systems are model-based, but model-independent strategies have been investigated as well, as in [7].

In this paper a Model-based Predictive Control (MPC) strategy is proposed for the simultaneous position and vibration control for flexible-link mechanisms. The available literature on the subject is quite limited to Authors' best knowledge. In [8] two MPC controllers are used to independently control the hub angular velocity and the angular tip position of a flexible beam. Hassan [9] reports the experimental analysis of a vibration suppression system by using piezoceramic actuators. In [10] a single-link mechanism is controlled by an MPC by using the angular hub position feedback, a tip-positioned load cell and an ultrasound tip displacement feedback. Other papers on this topics have been proposed by the Authors in [11], [12] on a single-link and a four-link flexible-link mechanism, respectively, using two predictive controllers based on state-space formulation. It should be pointed out that the works [8], [9], [10] are experimental investigation conducted on mechanisms that rotate on the horizontal plane, while this work involves a FLM affected by gravity.

In this paper the validity of previous numerical results are confirmed by the experimental tests. The test bench is a single-link flexible mechanism affected by gravity force. The performance of the proposed MPC is evaluated by comparing its closed-loop behavior to the one obtained trough a classical LQ control with an integral action. Moreover, an extended Kalman filter is used as a state observer. The estimation of the state of the plant is based only on the measure of the angular position of the hub and on the torque signal, thus reducing the effects of measures such as strain gauge signal which are usually affected by noise. The accuracy of such system is evaluated experimentally by comparing the estimated state with the measure of the elastic displacements evaluated by a strain gauge transducer.

II. Dynamic model of a flexible-link planar mechanism

In this section the dynamic model of a flexible-link mechanism suggested by Giovagnoni [13] will be briefly explained. The choice of this formulation among the several proposed in the last 30 years has been motivated by the high grade of accuracy provided by this model, which has been proved several times, for example in [3], [14].

The main characteristics of this model can be summarized in four points:

1. finite element (FEM) formulation
2. Equivalent Rigid-Link System (ERLS) formulation [15]
3. mutual dependence of the rigid and flexible motion

*paolo.boscariol@uniud.it

4. capability of describing mechanisms with an arbitrary number of flexible and rigid links

First, each flexible link of the mechanism is subdivided into several finite elements. Referring to the Figure 1 the following vectors, calculated in the global reference frame $\{X, Y, Z\}$, can be defined:

- $\mathbf{r}_i$ and $\mathbf{u}_i$ are the vectors of nodal position and nodal displacement in the i-th element of the ERLS
- $\mathbf{p}_i$ is the position of a generic point inside the i-th element
- $\mathbf{q}$ is the vector of generalized coordinates of the ERLS

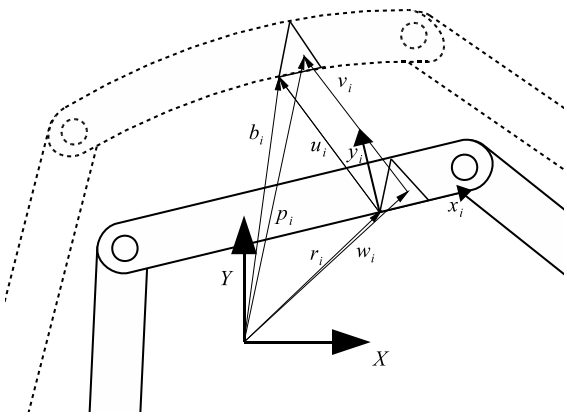

Fig. 1. Kinematic definitions

The vectors defined so far are calculated in the global reference frame $\{X, Y, Z\}$. Applying the principle of virtual work:

$$\delta W^{elastic} + \delta W^{external} + \delta W^{inertia} = 0$$

the following relation can be stated:

$$\begin{aligned}\sum_i \int_{V_i} \delta \mathbf{p}_i{}^T \ddot{\mathbf{p}}_i \rho_i dw + \sum_i \int_{V_i} \delta \epsilon_i{}^T \mathbf{D}_i \epsilon_i dw \\ = \sum_i \int_{V_i} \delta \mathbf{p}_i{}^T \mathbf{g} \rho dw + (\delta \mathbf{u}^T + \delta \mathbf{r}^T)\mathbf{F}\end{aligned} \tag{1}$$

ϵ_i, $\mathbf{D}_i$, ρ_i and $\delta\epsilon_i$ are the strain vector, the stress-strain matrix, the mass density of the i-th link and the virtual strains, respectively. $\mathbf{F}$ is the vector of the external forces, including the gravity, whose acceleration vector is $\mathbf{g}$. Eq. 1 shows the virtual works of inertial, elastic an external forces, respectively. From this equation, $\mathbf{p}_i$ and $\ddot{\mathbf{p}}_i$ for a generic point in the i-th element are:

$$\begin{aligned}\delta \mathbf{p}_i &= \mathbf{R}_i \mathbf{N}_i \mathbf{T}_i \delta \mathbf{r}_i \\ \ddot{\mathbf{p}}_i &= \mathbf{R}_i \mathbf{N}_i \mathbf{T}_i + 2(\dot{\mathbf{R}}_i \mathbf{N}_i \mathbf{T}_i + \mathbf{R}_i \mathbf{N}_i \dot{\mathbf{T}}_i)\dot{\mathbf{u}}_i\end{aligned} \tag{2}$$

where $\mathbf{T}_i$ is a matrix that describes the transformation from global-to-local reference frame of the i-th element, $\mathbf{R}_i$ is the local-to-global rotation matrix and $\mathbf{N}_i$ is the shape function matrix. Taking $\mathbf{B}_i(x_i, y_i, z_i)$ as the strain-displacement matrix, the following relation holds:

$$\begin{aligned}\epsilon_i &= \mathbf{B}_i \mathbf{T}_i \delta \mathbf{u}_i \\ \delta \epsilon_i &= \mathbf{B}_i \delta \mathbf{T}_i \mathbf{u}_i + \mathbf{B}_i \mathbf{T}_i \delta \mathbf{u}_i\end{aligned} \tag{3}$$

Since nodal elastic virtual displacements ($\delta\mathbf{u}$) and nodal virtual displacements of the ERLS ($\delta\mathbf{r}$) are independent from each other, from the relations reported above the resulting equation describing the motion of the system is:

$$\begin{bmatrix} \mathbf{M} & \mathbf{MS} \\ \mathbf{S}^T\mathbf{M} & \mathbf{S}^T\mathbf{MS} \end{bmatrix} \begin{bmatrix} \ddot{\mathbf{u}} \\ \ddot{\mathbf{q}} \end{bmatrix} = \begin{bmatrix} \mathbf{f} \\ \mathbf{S}^T\mathbf{f} \end{bmatrix} \tag{4}$$

$\mathbf{M}$ is the mass matrix of the whole system and $\mathbf{S}$ is the sensitivity matrix for all the nodes. Vector $\mathbf{f} = \mathbf{f}(\mathbf{u}, \dot{\mathbf{u}}, \mathbf{q}, \dot{\mathbf{q}})$ accounts for all the forces affecting the system, including the gravity force. Adding a Rayleigh damping, the right-hand side of Eq. 4 becomes:

$$\begin{aligned}\begin{bmatrix} \mathbf{f} \\ \mathbf{S}^T\mathbf{f} \end{bmatrix} = \\ \begin{bmatrix} -2\mathbf{M}_g - \alpha\mathbf{M} - \beta\mathbf{K} & -\mathbf{M}\dot{\mathbf{S}} & -\mathbf{K} \\ \mathbf{S}^T(-2\mathbf{M}_G - \alpha\mathbf{M}) & -\mathbf{S}^T\mathbf{M}\dot{\mathbf{S}} & 0 \end{bmatrix} \begin{bmatrix} \dot{\mathbf{u}} \\ \dot{\mathbf{q}} \\ \mathbf{u} \end{bmatrix} \\ + \begin{bmatrix} \mathbf{M} & \mathbf{I} \\ \mathbf{S}^T\mathbf{M} & \mathbf{S}^T \end{bmatrix} \begin{bmatrix} \mathbf{g} \\ \mathbf{f} \end{bmatrix}\end{aligned} \tag{5}$$

Matrix $\mathbf{M}_G$ accounts for the Coriolis contribution, while $\mathbf{K}$ is the stiffness matrix of the whole system. α and β are the two Rayleigh damping coefficients. System in (4) and (5) can be made solvable by forcing to zero as many elastic displacement as the generalized coordinates, in this way ERLS position is defined univocally. Therefore removing the displacement forced to zero from (4) and (5) gives:

$$\begin{bmatrix} \mathbf{M}_{in} & (\mathbf{MS})_{in} \\ (\mathbf{S}^T\mathbf{M})_{in} & \mathbf{S}^T\mathbf{MS} \end{bmatrix} \begin{bmatrix} \ddot{\mathbf{u}}_{in} \\ \ddot{\mathbf{q}} \end{bmatrix} = \begin{bmatrix} \mathbf{f}_{in} \\ \mathbf{S}^T\mathbf{f} \end{bmatrix} \tag{6}$$

The values of the accelerations can be computed at each step by solving the system in Eq. 6, while the values of velocities and displacements can be obtained by an appropriate integration scheme (e.g. the Runge-Kutta algorithm). It is important to focus the attention on the size and the rank of the matrices involved in Eq. 6, and also to the choice of the general coordinates used in the ERLS definition. Otherwise it might happen that a singular configuration is encountered during the motion of the mechanism [13]. In this case, Eq. 6 cannot be solved.

III. Experimental setup

The plant used to evaluate the effectiveness of the proposed predictive control strategy is a single-link flexible mechanism. It is made by a long and thin steel rod, actuated by a brushless motor. No reduction gears are used, so one end of the link is rigidly coupled to the motor shaft. The flexible link can rotate on the vertical plane, so the mechanism dynamics is heavily affected by the gravity force. The

structural and dynamic characteristics of the flexible rod can be found in Table I. Owing to the overall dimensions, the mechanism has a limited movement range (around ± 25 [deg]) from the vertical position. The motion of the link is governed trough an Indramat DKC-MKD brushless servo drive system. This drive is used as a torque generator, i.e. the instant value of the torque applied by the motor can be controlled by using an analog signal. Such a signal is supplied by a National Instruments PCI-6259 DAQ board, controlled by a Core 2 Quad PC. The angular position is measured by a 4000 cpr quadrature encoder is read with a National Instruments PCI-6602 board. The strain gauge signal is measured with the same PCI-6259 board used to generate the torque reference signal, as it is visible in Figure 4. The data acquisition and the control softwares run over the LabVIEW Real-Time OS.

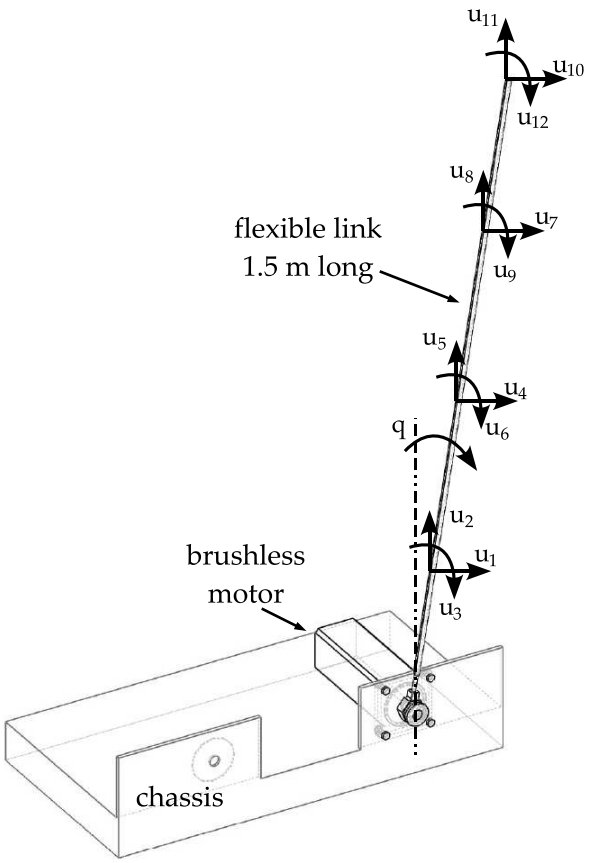

Fig. 2. The finite element discretization

The dynamic model can be described with a good accuracy it with four finite elements. This discretization is sufficient to describe accurately the first four modes of vibration: 23 Hz, 63 Hz, 124 Hz, 206 Hz. Higher order modes can be neglected as they have low energy and high damping values.

Fig. 3. The flexible-link mechanism used for experimental tests

Parameter		*Value*
Young's modulus	E	230×10^9 [Pa]
Flexural stiffness	EJ	191.67 [Nm^4]
Beam width	a	1×10^{-2} [m]
Beam thickness	b	1×10^{-2} [m]
Mass/unit length	m	0.7880 [kg/m]
Flexible Link length	l	1.5 [m]
Strain sensor position	s	0.75 [m]
1st Rayleigh damp. const.	α	4.5×10^{-1} [s^{-1}]
2nd Rayleigh damp. const.	β	4.2×10^{-5} [s^{-1}]

TABLE I. Structral and dynamics characteristics of the flexible rod

IV. Model Predictive Control

In this section a brief explanation of the MPC used for experimental tests is given. Further details can be found in [16] and [17]. MPC refers to a class of controllers which compute an optimal control sequence by using the concepts of:

- internal prediction model
- receding horizon principle
- constrained optimization

Given a MIMO plant described by a discrete-time state space model, k can be defined as the discrete time variable. Let $\mathbf{z}(k)$, $\mathbf{y}(k)$, $\mathbf{x}(k)$ and $\mathbf{r}(k)$ be the input, the output, the state and the reference vectors, respectively. The discrete

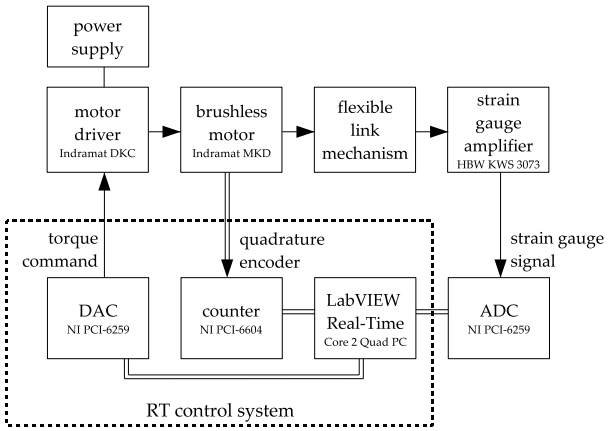

Fig. 4. Experimental setup

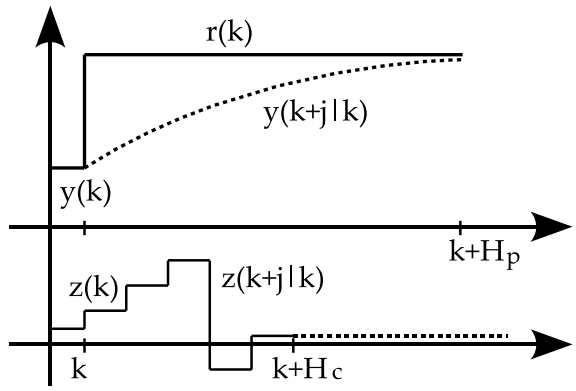

Fig. 5. Receding horizon principle

state space LTI system is described by the triplet $(\mathbf{A}, \mathbf{B}, \mathbf{C})$:

$$\begin{aligned} \mathbf{x}(k+1) &= \mathbf{A}\mathbf{x}(k) + \mathbf{B}\mathbf{z}(k) \\ \mathbf{y}(k) &= \mathbf{C}\mathbf{x}(k) \end{aligned} \tag{7}$$

First of all, the state space model is converted to the equivalent incremental form. Therefore, instead of eq. (7), the following set of equations are used to describe the dynamics of the plant:

$$\begin{aligned} &\overbrace{\begin{bmatrix} \Delta\mathbf{x}(k+1) \\ \mathbf{y}(k+1) \end{bmatrix}}^{\mathbf{x}'(k+1)} = \overbrace{\begin{bmatrix} \mathbf{A} & 0 \\ \mathbf{CA} & \mathbf{I} \end{bmatrix}}^{\mathbf{A}'} \overbrace{\begin{bmatrix} \Delta\mathbf{x}(k) \\ \mathbf{y}(k) \end{bmatrix}}^{\mathbf{x}'(k)} \\ &+ \underbrace{\begin{bmatrix} \mathbf{B} \\ \mathbf{CB} \end{bmatrix}}_{\mathbf{B}'} \Delta\mathbf{z}(k) \\ &\mathbf{y}(k) = \underbrace{\begin{bmatrix} 0 & \mathbf{I} \end{bmatrix}}_{\mathbf{C}'} \begin{bmatrix} \Delta\mathbf{x}(k) \\ \mathbf{y}(k) \end{bmatrix} \end{aligned} \tag{8}$$

The triplet $(\mathbf{A}', \mathbf{B}', \mathbf{C}')$ describes the behavior of the plant in terms of the increments $\Delta\mathbf{x}(k) = \mathbf{x}(k+1) - \mathbf{x}(k)$, $\Delta\mathbf{z}(k) = \mathbf{z}(k) - \mathbf{z}(k-1)$ and $\mathbf{y}(k)$. For sake of simplicity, in the following the triplet $(\mathbf{A}', \mathbf{B}', \mathbf{C}')$ and the vector $\mathbf{x}'(k)$ will be indicated without the apex " $'$ ".

At each time k-th, the proposed MPC controller computes the sequence of increments for the control variable vector $\Delta\mathcal{Z}(k)$, whose length is of H_c steps. Such a length is called *control horizon*, and the elements of $\Delta\mathcal{Z}(k)$ are:

$$\Delta\mathcal{Z}(k) = [\Delta\mathbf{z}(k+1|k), \Delta\mathbf{z}(k+2|k), \ldots, \Delta\mathbf{z}(k+H_c|k)]^T \tag{9}$$

$\Delta\mathcal{Z}(k)$ is calculated in order to minimize the predicted control effort and the predicted distance from the reference trajectory of the controlled variables over a period, which is called *prediction horizon*, indicated as H_p. Usually $H_c \leq H_p$. The receding horizon principle (as in Fig. 5) states that the evaluation of the correct control action is performed at every time instant k, but only the first value of such a vector is supplied to the plant at time k. At the following iteration $k+1$, another $\Delta\mathcal{Z}$ is computed, and again only the first value is applied, and so on, for all the following iterations. Such technique is referred to as receding horizon, since the control and prediction horizon "slide" forward in time at every time step.

By using the previous notation , the sequence of predicted values of the state vector $\mathbf{x}(k)$ and the plant output $\mathbf{y}(k)$ can be expressed as:

$$\mathcal{X}(k) = [\mathbf{x}(k+1|k), \mathbf{x}(k+2|k), \ldots, \mathbf{x}(k+H_p|k)]^T \tag{10}$$

$$\mathcal{Y}(k) = [\mathbf{y}(k+1|k), \mathbf{y}(k+2|k), \ldots, \mathbf{y}(k+H_p|k)]^T \tag{11}$$

Assuming that the whole state vector $\mathbf{x}(k)$ is available at any time, its future evolution can be estimated by iterating eq. (8) as follows:

$$\begin{aligned} \mathbf{x}(k+1|k) &= \mathbf{A}\mathbf{x}(k) + \mathbf{B}\Delta\mathbf{z}(k) \\ \mathbf{x}(k+2|k) &= \mathbf{A}\mathbf{x}(k+1|k) + \mathbf{C}\Delta\mathbf{z}(k+1) \\ &= \mathbf{A}^2\mathbf{x}(k) + \mathbf{AB}\Delta\mathbf{z}(k) + \mathbf{B}\Delta\mathbf{z}(k+1) \\ &\vdots \\ \mathbf{x}(k+H_p|k) &= \mathbf{A}^{H_p}\mathbf{x}(k) + \mathbf{A}^{H_p-1}\mathbf{B}\Delta\mathbf{z}(k) \\ &\quad + \mathbf{A}^{H_p-2}\mathbf{B}\Delta\mathbf{z}(k+1) \\ &\quad + \ldots + \mathbf{A}^{H_p-H_c}\mathbf{B}\Delta\mathbf{z}(k+H_c-1) \end{aligned} \tag{12}$$

The future evolution of the output vector $\mathbf{y}(k+j|k)$ with $j = 1, 2, \ldots, H_p$ is directly linked to the evaluation of $\mathbf{x}(k+j|k)$ by the equation:

$$\mathbf{y}(k+j|k) = \mathbf{C}\mathbf{x}(k+j|k) \quad with \quad j = 1, 2, \ldots, H_p \tag{13}$$

Equation (13) can also be expressed as:

$$\mathcal{Y}(k) = \mathbf{\Gamma}\mathbf{x}(k) + \mathbf{\Phi}\Delta\mathcal{Z}(k) \tag{14}$$

with:

$$\mathbf{\Gamma} = \begin{bmatrix} \mathbf{CA} \\ \mathbf{CA}^2 \\ \vdots \\ \mathbf{CA}^{H_p} \end{bmatrix}$$

$$\mathbf{\Phi} = \begin{bmatrix} \mathbf{CB} & 0 & 0 & \dots & 0 \\ \mathbf{CAB} & \mathbf{CB} & 0 & \dots & 0 \\ \mathbf{CA}^2\mathbf{B} & \mathbf{CAB} & \mathbf{CB} & \dots & 0 \\ \vdots & & & & \\ \mathbf{CA}^{H_p-1}\mathbf{B} & \mathbf{CA}^{H_p-2}\mathbf{B} & \mathbf{CA}^{H_p-2}\mathbf{B} & \dots & \mathbf{CA}^{H_p-H_c}\mathbf{B} \end{bmatrix}$$

The MPC controller implemented for the experimental tests calculates the optimal value of the incremental input trajectory $\Delta\mathcal{Z}(k)$ as the minimum of the cost function:

$$J_{MPC}(k) = \sum_{i=1}^{H_p} \|\mathbf{y}(k) - \mathbf{r}(k)\|^2_{\mathbf{Q}} + \sum_{i=0}^{H_c-1} \|\Delta\mathbf{z}(k)\|^2_{\mathbf{R}} \tag{15}$$

in which $\mathbf{Q}$ and $\mathbf{R}$ are diagonal matrices of the suitable weights. The minimization of cost function J_{MPC} can be solved with the following constraints on the i-th value of the state vector $\mathbf{x}$, the control variables $\mathbf{z}$ and its change rate $\Delta\mathbf{z}$:

$$\begin{aligned} x_i^{\min} \le x_i \le x_i^{\max} \\ z_i^{min} \le z_i \le z_i^{max} \\ \Delta z_i^{min} \le \Delta z_i \le \Delta z_i^{max} \end{aligned} \tag{16}$$

In this way, the sequence of optimal values $\mathcal{Z}(k)$ can be found using a numeric procedure, such as quadratic programming, see [16].

V. State observer

The control strategy explained above can be applied only when a measure of the whole state $\mathbf{x}$ is available. In this application, there are only two measured values, so a state observer must be used. Here a Kalman asymptotic estimator has been chosen. An estimation of $\mathbf{x}(k)$ and $\mathbf{x}_m(k)$ (where $\mathbf{x}(k)$ is the state of the plant model and $\mathbf{x}_m(k)$ is the state of the measurement noise model) can be computed from the measured output $\mathbf{y}_m(k)$ as:

$$\begin{aligned} \begin{bmatrix} \hat{\mathbf{x}}(k|k) \\ \hat{\mathbf{x}}_m(k|k) \end{bmatrix} &= \begin{bmatrix} \hat{\mathbf{x}}(k|k-1) \\ \hat{\mathbf{x}}_m(k|k-1) \end{bmatrix} + \mathbf{L}(\mathbf{y}_m(k) - \hat{\mathbf{y}}_m(k)) \\ \begin{bmatrix} \hat{\mathbf{x}}(k+1|k) \\ \hat{\mathbf{x}}_m(k+1|k) \end{bmatrix} &= \begin{bmatrix} \mathbf{A}\hat{\mathbf{x}}(k|k) + \mathbf{B}\mathbf{z}(k) \\ \tilde{\mathbf{A}}\hat{\mathbf{x}}_m(k|k) \end{bmatrix} \\ \hat{\mathbf{y}}_m(k) &= \mathbf{C}_m\hat{\mathbf{x}}(k|k-1) \end{aligned} \tag{17}$$

The gain matrix $\mathbf{L}$ has been designed by using Kalman filtering techniques (see [18]).

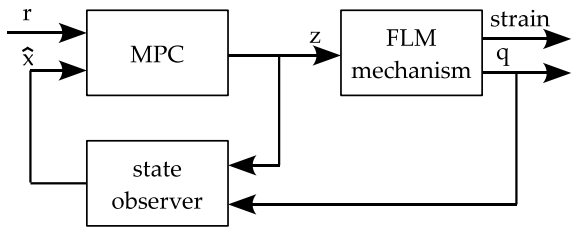

Fig. 6. MPC control: block diagram

The dynamic model represented by Eq. 6 is strongly nonlinear, due to the quadratic relation between the nodal accelerations and the velocities of the free coordinates, and to the effects of the gravity force. Thus it cannot be used as a prediction model for a linear MPC controller or as the basis of a Kalman state observer. In order to develop a state-space form linearized version of the dynamic system of (6) a linearization procedure has been developed by Gasparetto in [19]. Here this procedure will be briefly recalled.

From the basics of system theory, a linear time-invariant model expressed in state-space can be written as:

$$\begin{cases} \dot{\mathbf{x}}(t) = \mathbf{A}\mathbf{x}(t) + \mathbf{B}\mathbf{z}(t) \\ \mathbf{y}(t) = \mathbf{C}\mathbf{x}(t) + \mathbf{D}\mathbf{x}(t) \end{cases} \tag{18}$$

where $\mathbf{x}(t)$ is the state vector, $\mathbf{y}(t)$ is the output vector, $\mathbf{z}(t)$ represents the input vector and $\mathbf{A}$, $\mathbf{B}$, $\mathbf{C}$ and $\mathbf{D}$ are time-invariant matrices. Taking $\mathbf{x} = [\dot{\mathbf{u}}, \dot{\mathbf{q}}, \mathbf{u}, \mathbf{q}]^T$ as the state vector, linearized state-space form of the dynamic model in Eq.6 can be written as:

$$\mathcal{A}_{lin}\dot{\mathbf{x}} = \mathcal{B}_{lin}\,\mathbf{x} + \mathcal{C}_{lin}\tau \tag{19}$$

Now a steady "equilibrium" configuration $\mathbf{x}_e$ where $\mathbf{u} = \mathbf{u}_e$ under the system input $\mathbf{z} = \mathbf{z}_e$ can be chosen. In the neighborhood of this point holds:

$$\begin{cases} \mathbf{x}(t) = \mathbf{x}_e + \Delta\mathbf{x}(t) \\ \mathbf{z}(t) = \mathbf{z}_e + \Delta\mathbf{z}(t) \end{cases} \tag{20}$$

So, bringing these relations into Eq. 6, the following relationship turns out:

$$\begin{aligned} \mathcal{A}_{lin}(\mathbf{x}_e)\Delta\dot{\mathbf{x}} = \mathcal{B}_{lin}(\mathbf{x}_e + \Delta\mathbf{x})(\mathbf{x}_e + \Delta\mathbf{x}) \\ + \mathcal{C}_{lin}(\mathbf{x}_e + \Delta\mathbf{x})(\mathbf{z}_e + \Delta\mathbf{z}) \end{aligned} \tag{21}$$

After some steps that can be found in more detail in [19], $\mathcal{A}_{lin}$ and $\mathcal{B}_{lin}$ matrices in (19) can be written as:

$$\mathcal{A}_{lin} = \begin{bmatrix} \mathbf{M} & \mathbf{MS} & 0 & 0 \\ \mathbf{S}^T\mathbf{M} & \mathbf{S}^T\mathbf{MS} & 0 & 0 \\ 0 & 0 & \mathbf{I} & 0 \\ 0 & 0 & 0 & \mathbf{I} \end{bmatrix} \tag{22}$$

$$\mathcal{B}_{lin} = \begin{bmatrix} -2\mathbf{M}_G - \alpha\mathbf{M} - \beta\mathbf{K} & 0 & -\mathbf{K} & \mathbf{B}_{14} \\ \mathbf{S}^T(-2\mathbf{M}_G - \alpha\mathbf{M} - \beta\mathbf{K}) & 0 & 0 & \mathbf{B}_{24} \\ \mathbf{I} & 0 & 0 & 0 \\ 0 & \mathbf{I} & 0 & 0 \end{bmatrix} \tag{23}$$

where:

$$\mathbf{B}_{14} = -\left.\frac{\partial \mathbf{K}}{\partial \mathbf{q}}\right|_{\mathbf{q}=\mathbf{q}_e} \cdot \mathbf{u}_e + \left.\frac{\partial \mathbf{f}}{\partial \mathbf{q}}\right|_{\mathbf{q}=\mathbf{q}_e}$$

and:

$$\mathbf{B}_{24} = \left.\frac{\partial\left(\mathbf{S}^T\mathbf{f}\right)}{\partial \mathbf{q}}\right|_{\mathbf{q}=\mathbf{q}_e}.$$

$\mathcal{C}_{lin}$ remains unchanged after the linearization process, since it is composed of only zeros and ones. The standard form of the state-space system can be easily found from $\mathcal{A}_{lin}$, $\mathcal{B}_{lin}$ and $\mathcal{C}_{lin}$:

$$\begin{aligned} \Delta\dot{\mathbf{x}} &= \mathbf{A}\Delta\mathbf{x} + \mathbf{B}\Delta\mathbf{z} \\ \mathbf{y} &= \mathbf{C}\mathbf{x} + \mathbf{D}\mathbf{z} \end{aligned} \tag{24}$$

where:

$$\begin{aligned} \mathbf{A} &= \mathcal{A}_{lin}{}^{-1}\mathcal{B}_{lin} \\ \mathbf{B} &= \mathcal{A}_{lin}{}^{-1}\mathcal{C}_{lin} \end{aligned} \tag{25}$$

where $\mathbf{A} \in \mathbb{R}^{26} \times \mathbb{R}^{26}$, $\mathbf{B} \in \mathbb{R}^{26} \times \mathbb{R}^{1}$, $\mathbf{C} \in \mathbb{R}^{2} \times \mathbb{R}^{26}$ are time-invariant matrices. The state vector $\mathbf{x}$ includes all the nodal displacements and the angular position q, as well as their time derivatives:

$$\mathbf{x}(t) = [u_1, u_2, \ldots, u_{12}, q, \dot{u_1}, \dot{u_2}, \ldots, \dot{u}_{12}, \dot{q}]^T$$

The output vector of the LTI system consists of two elements: $\mathbf{y}(t) = [u_6, q]^T$, being u_6 the rotational displacement at the midspan of the link. The input vector $\mathbf{z}(t)$ includes the torque applied to the link as single element.

A comparison of measured and estimated values of the link curvature is reported in Figures 7 and 8. As it can be seen, the value of the elastic displacement can be evaluated with a good accuracy. It must be pointed out that the state observer has the availability of only the quadrature encoder signal and the nominal torque applied to the rod. In this way, the robustness of the closed-loop system can be improved, since the measure of the strain gauge signal is heavily affected by noise. Moreover, the reduced number of sensor make this control strategy suitable to most robotic manipulators for industrial use, since sensors such as accelerometers and strain gauge bridges are usually unavailable on these systems.

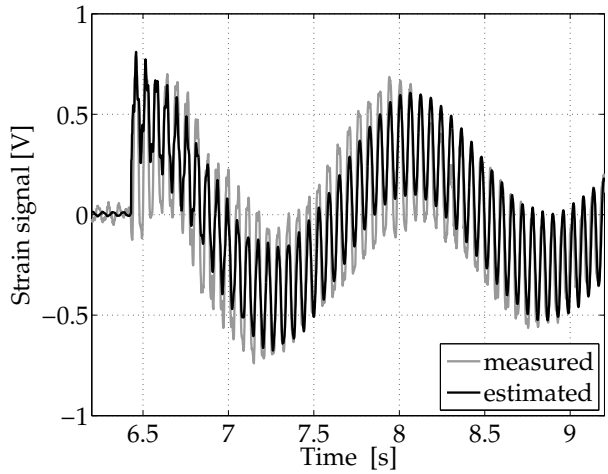

Fig. 7. State observer: measured and estimated strain gauge signals

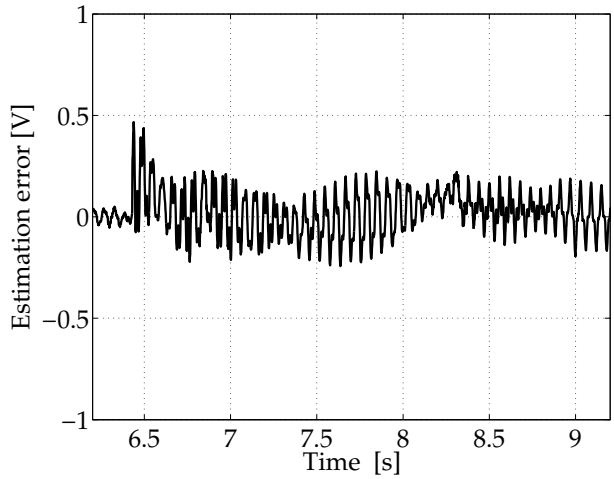

Fig. 8. State observer: estimation error

VI. Experimental results: MPC control

The proof of the accuracy of the controller is given in this section. The position regulation and the vibration damping are evaluated from the results of two different experimental tests. In the first test, indicated as "Test 1" in Table II and in Figures 9,10,11, the reference angular position signal is an ideal step that decreases form $+15$ [deg] to -15 [deg]. As it can be seen in Figure 9 the 30-degrees movement is performed in 2 seconds, with a very small overshoot and without any steady state error. As it is clear form Figure 11, the value of the torque command is kept inside the allowable range of the actuator. The closed-loop system shows a good damping, since the vibration is kept below the minimum detectable amplitude within 3 seconds from the transient. Vibration damping can be improved at the cost of a scarce degradation of the accuracy on the angular position accuracy. In "Test 2" the weight on the angular position, $\mathbf{Q}(1,1)$, is reduced by 33 %, while the weight on vibra-

TABLE II. MPC tuning parameters

	Test 1	*Test 2*
q_0 $[deg]$	15	-15
q_f $[deg]$	-10	10
H_p	400	500
H_c	10	10
$\mathbf{Q}(1,1)$	300	200
$\mathbf{Q}(2,2)$	3000	4000
$\mathbf{R}$	1	1

tion amplitude, $\mathbf{Q}(2,2)$ is increased by 33 %, with respect to "Test 1". At the same time, the prediction horizon is changed from 400 to 500. The increasing of H_p leads to a more damped response, and can improve the robustness of the system, as highlighted in [12]. Moreover, the vibration damping can be enhanced by increasing the weight on u and reducing the weight on q. As it is evident form Figure 12, the tracking of the angular position is less fast, but the overshoot is reduced. Vibration damping is slightly improved from Test 1, as it can be seen in Figure 13. In the Test 2 the range of the position reference is reduced to 20 degrees to show how the performance of the MPC controller is not affected by the width of the reference step signal.

In all the tests, the angular position is evaluated by the quadrature encoder mounted on the motor shaft, while the strain signal is measured using a Hottinger Baldwin Messtechnik KWS 3073 strain gauge signal amplifier, as in Figure 4.

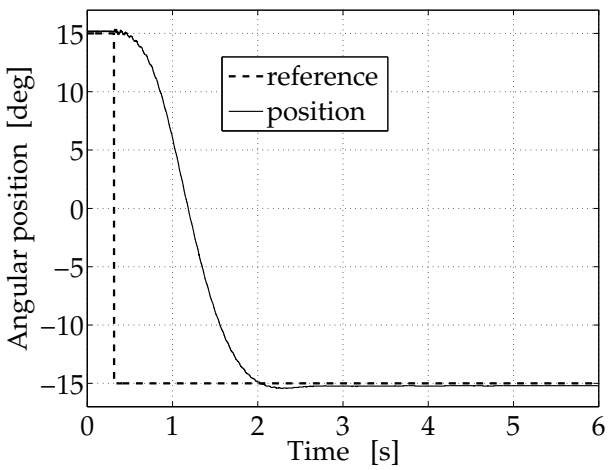

Fig. 9. MPC control: closed-loop response to a step position reference, angular position q. Test 1

VII. Experimental results: comparison between MPC and LQ performance

In this section the performance of the proposed MPC controlled are evaluated by comparing them with those of a Liner Quadratic controller with an integral action. All the tests have been conducted by providing the angular position reference signal with ideal steps of different amplitudes.

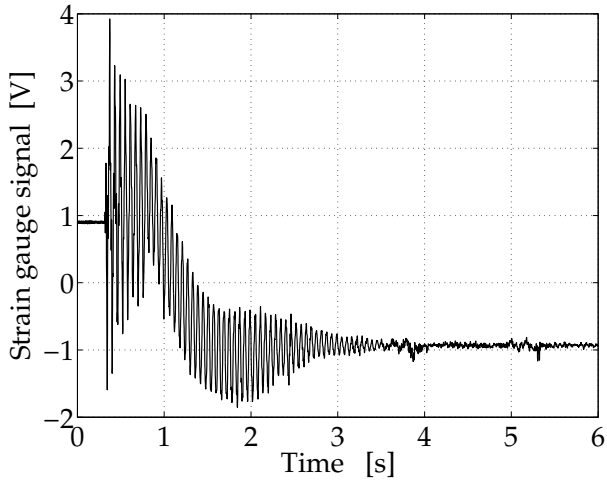

Fig. 10. MPC control: closed-loop response to a step position reference, strain gauge signal. Test 1

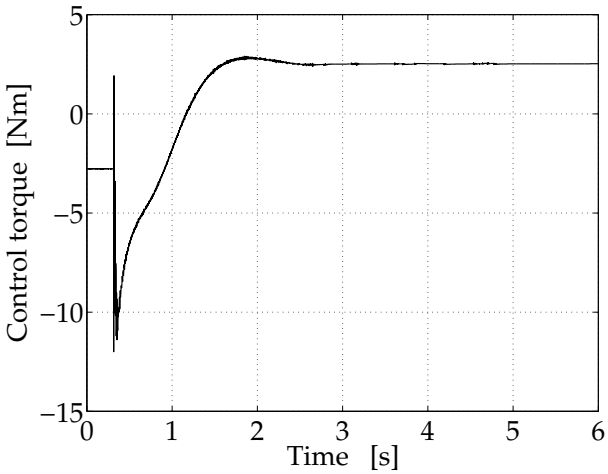

Fig. 11. MPC control: closed-loop response to a step position reference, applied torque. Test 1

Here just a brief overview of the Linear Quadratic (LQ) control strategy for flexible link mechanism is given. Such a controller is used to set up a comparison between the MPC controller and a classic control system based on the same model and the same controlled variables. In this way the features of the predictive control strategy can be clearly highlighted.

A graphic representation of the control's loop structure is reported in Figure 15. Owing to the space constraints of this paper, just a basic overview of this controller will be given (for more details see [20]).

In order to add an integral action into the LQ controller, the state-space model must be augmented. The tracking error can be defined so that its time derivative obeys to the following differential equation:

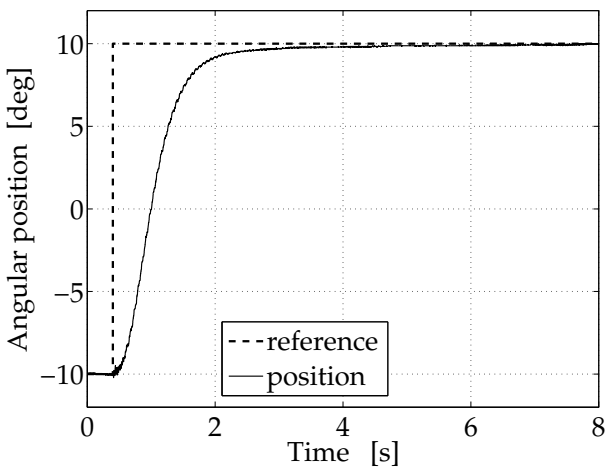

Fig. 12. MPC control: closed-loop response to a step position reference, angular position q. Test 2

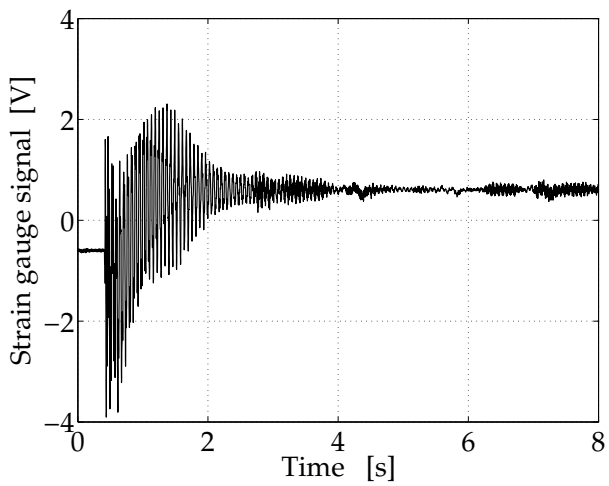

Fig. 13. MPC control: closed-loop response to a step position reference, strain gauge signal. Test 2

$$\dot{\mathbf{w}}(t) = \mathbf{r}(r) - \mathbf{y}(t) = \mathbf{r}(t) - \mathbf{C}\mathbf{x}(t) \tag{26}$$

where $\mathbf{r}(t)$ is the desired trajectory that the plant output $\mathbf{y}(t)$ should follow. In this way, $\mathbf{w}(t)$ is the integral of the tracking error. An augmented state vector $\hat{\mathbf{x}}$ can be defined such as: $\hat{\mathbf{x}} = \begin{bmatrix} \mathbf{x} \\ \mathbf{w} \end{bmatrix}$, then the augmented state equation is:

$$\dot{\hat{\mathbf{x}}}(t) = \underbrace{\begin{bmatrix} \mathbf{A} & 0 \\ -\mathbf{C} & 0 \end{bmatrix}}_{\hat{\mathbf{A}}} \hat{\mathbf{x}} + \underbrace{\begin{bmatrix} \mathbf{B} \\ 0 \end{bmatrix}}_{\hat{\mathbf{B}}} \mathbf{z} + \underbrace{\begin{bmatrix} 0 \\ \mathbf{r} \end{bmatrix}}_{\mathbf{d}} \tag{27}$$

while the augmented output equation is:

$$\mathbf{y} = \underbrace{\begin{bmatrix} \mathbf{C} & 0 \end{bmatrix}}_{\hat{\mathbf{C}}} \hat{\mathbf{x}} \tag{28}$$

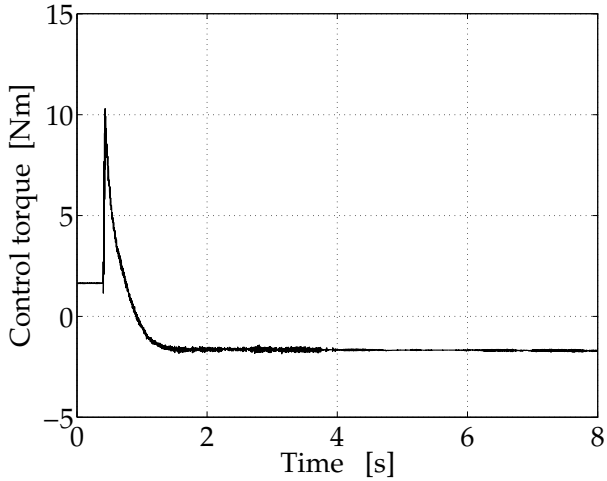

Fig. 14. MPC control: closed-loop response to a step position reference, applied torque. Test 2

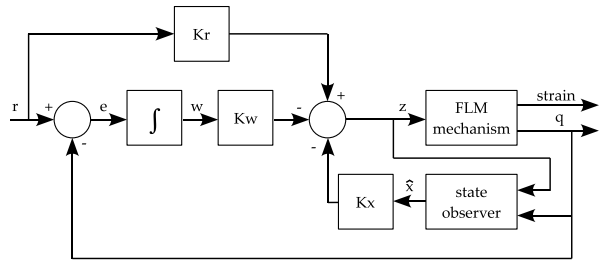

Fig. 15. LQ control with integral action: block diagram

The LQ tracking controller calculates the optimal control sequence $\mathbf{z}(t)$ which minimizes the performance index J defined as:

$$J = \frac{1}{2} \int_0^\infty \left\{ (\mathbf{y} - \mathbf{r})^T \mathbf{Q}_y (\mathbf{y} - \mathbf{r}) + \mathbf{w}^T \mathbf{Q}_w \mathbf{w} + \mathbf{z}^T \mathbf{R} \mathbf{z} \right\} dt \tag{29}$$

The first term inside the integral minimizes the absolute value of the tracking error and the elastic displacement. Whereas, the second term takes into account the absolute value of integral error of q. The last one minimizes the system input: in this case the torque applied to the link.

In this case $\mathbf{Q}_y$ is a diagonal matrix of weights, while $\mathbf{Q}_w$ and $\mathbf{R}$ are scalar values. The control action obeys to:

$$z(t) = -\mathbf{K}_x \mathbf{x} - \mathbf{K}_w w + \mathbf{K}_r \mathbf{r} \tag{30}$$

where the optimal value of the gain matrices $\mathbf{K}_x, \mathbf{K}_w, \mathbf{K}_r$ are found trough the solution of a suitable Riccati equation.

Here, a comparison of the closed loop performance by using the LQ and the MPC controller is set. The two control systems are tuned to obtain the same rise time. As it can be seen from Figure 16, the LQ control has a poor accuracy on the position tracking: the overshoot is 1.3 degrees wide

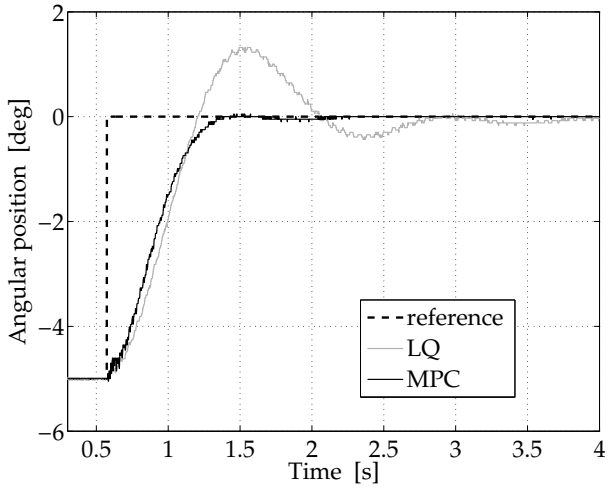

Fig. 16. LQ vs MPC: comparison of angular position tracking

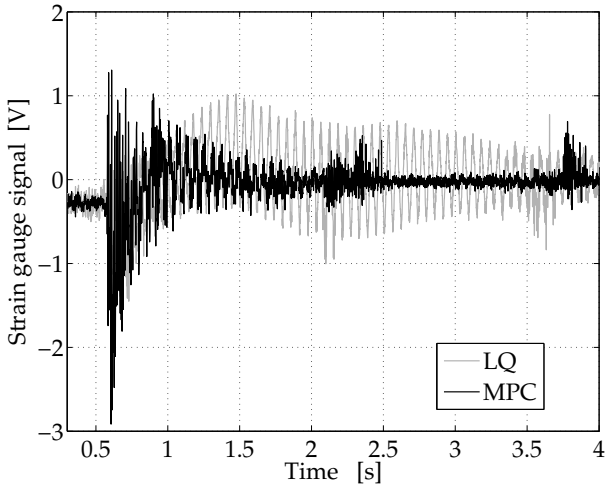

Fig. 17. LQ vs MPC: comparison of strain gauge signal

and the settling time is more or less 3 seconds long. The improved angular tracking error of MPC is highlighted by the much smaller settling time (less than 1 second) and by the negligible overshoot, as it can be seen in Figure 17.

As far as the vibration damping is concerned, the MPC again performs better: the elastic displacement is kept below the minimum detectable amplitude range ± 70 [mV] after less than 2 seconds from the change in reference, while the same occurs for the LQ controller after more than 5 seconds. The comparison between the two controllers is limited to a 5-degree-wide step, since the LQ controller cannot preserve satisfactory performance over this reference step without a strong slowing down of the closed-loop response of the system. The strain signal is very noisy. Figure 17 shows how the strain signal if affected by a periodic disturbance which occurs every 1.2 seconds. This disturbance is due mainly to the noise irradiated from the motor power supply and by the motor driver. It must be pointed out that this large amount of disturbance does not affect the performance of neither the LQ nor the MPC controller, since the state estimator used in both cases does not rely on this measurement.

Figure 18 shows the comparison of the two control torque profiles. It is visible how the LW control systems behaves just like a PID control with an high proportional gain. In fact it can be noticed how the amplitude of the control torque is directly proportional to the angular position error. On the other hand the control profile provided by the MPC controlled is very different, as it is composed by a sequence of short peaks and of a smooth profile.

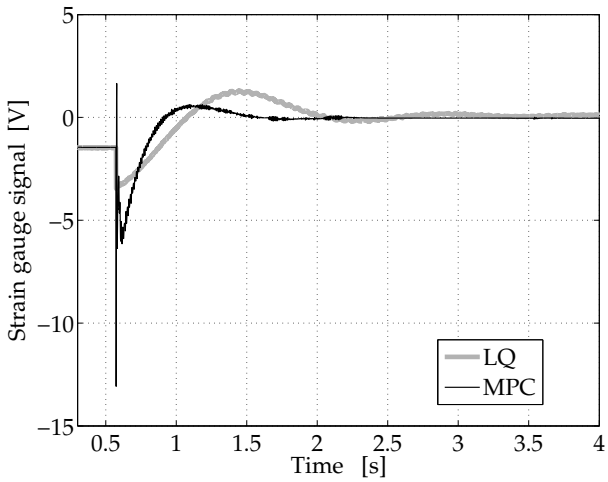

Fig. 18. LQ vs MPC: comparison of applied torques

VIII. Conclusion

In this paper the experimental validation of an MPC controller for the simultaneous position and vibration control of flexible-link mechanisms has been presented. The effectiveness of the proposed approach has been tested on a laboratory prototype. It has been shown that the Model Predictive Control outperforms classical control strategies based on the same dynamic model, such as the Linear Quadratic (LQ) optimal control, both in terms of angular position tracking and vibration damping.

The state estimator used for all the experimental tests has been shown to be capable of providing an accurate estimation of the plant dynamics with a very limited set of sensors. Such an estimator needs only the measure of the angular position and of the torque command supplied to the brushless motor, increasing the robustness and the field of application. For this reason the proposed controller can be easily adapted to most industrial manipulators, which usually do not have sensors for measuring the elastic displacement of the links.

References

[1] S. Dwivedy and P. Eberhard, "Dynamic analysis of flexible manipulators, a literature review," *Mechanism and Machine Theory*, vol. 41, no. 7, pp. 749–777, 2006.

[2] M. Benosman and G. Le Vey, "Control of flexible manipulators: A survey," *Robotica*, vol. 22, no. 05, pp. 533–545, 2004.

[3] R. Caracciolo, D. Richiedei, A. Trevisani, and V. Zanotto, "Robust mixed-norm position and vibration control of flexible link mechanisms," *Mechatronics*, vol. 15, no. 7, pp. 767–791, 2005.

[4] N. Chalhoub, G. Kfoury, and B. Bazzi, "Design of robust controllers and a nonlinear observer for the control of a single-link flexible robotic manipulator," *Journal of Sound and Vibration*, vol. 291, no. 1-2, pp. 437–461, 2006.

[5] A. Özer, E. Semercigil, *et al.*, "An event-based vibration control for a two-link flexible robotic arm: Numerical and experimental observations," *Journal of Sound and Vibration*, vol. 313, no. 3-5, pp. 375–394, 2008.

[6] X. Jiang, A. Konno, and M. Uchiyama, "Vision-Based Task-Level Control of a Flexible-Link Manipulator," *Advanced Robotics*, vol. 24, no. 4, pp. 467–488, 2010.

[7] W. Chatlatanagulchai, P. Meckl, and M. ASME, "Model-Independent Control of a Flexible-Joint Robot Manipulator," *Journal of Dynamic Systems, Measurement, and Control*, vol. 131, p. 041003, 2009.

[8] K. Zmeu and E. Shipitko, "Predictive controller design with offline model learning for flexible beam control," in *Physics and Control, 2005. Proceedings. 2005 International Conference*, pp. 345–350, 2005.

[9] M. Hassan, R. Dubay, C. Li, and R. Wang, "Active vibration control of a flexible one-link manipulator using a multivariable predictive controller," *Mechatronics*, vol. 17, no. 6, pp. 311–323, 2007.

[10] T. Fan and C. De Silva, "Dynamic modelling and model predictive control of flexible-link manipulators," *International Journal of Robotics and Automation*, vol. 23, no. 4, pp. 227–234, 2008.

[11] P. Boscariol, A. Gasparetto, and V. Zanotto, "Vibration reduction in a flexible link mechanism through the synthesis of an mpc controller," in *Proceedings of the 5th IEEE Iternational Conference on Mechatronics (ICM2009)*, (Malaga, Spain), 14-17 April 2009.

[12] P. Boscariol, A. Gasparetto, and V. Zanotto, "Active position and vibration control of a flexible links mechanism using model-based predictive control," *Journal of Dynamic Systems, Measurement, and Control*, vol. 132, January 2010.

[13] M. Giovagnoni, "A numerical and experimental analysis of a chain of flexible bodies," *Journal of Dynamic Systems, Measurement, and Control*, vol. 116, pp. 73–80, 1994.

[14] A. Gasparetto, "On the modeling of flexible-link planar mechanisms: experimental validation of an accurate dynamic model," *Journal of dynamic systems, measurement, and control*, vol. 126, p. 365, 2004.

[15] L. Chang and J. Hamilton, "The kinematics of robotic manipulators with flexible links using an equivalent rigid link system (ERLS) model," *Journal of Dynamic Systems, Measurement, and Control*, vol. 113, p. 48, 1991.

[16] J. Maciejowski, *Predictive Control with Constraints*. Prentice Hall. Harlow, UK., 2001.

[17] L. Wang, *Model Predictive Control System Design and Implementation using MATLAB*. Springer Verlag, 2009.

[18] G. Franklin, M. Workman, and D. Powell, *Digital control of dynamic systems*. Addison-Wesley Longman Publishing Co., Inc. Boston, MA, USA, 1997.

[19] A. Gasparetto, "Accurate modelling of a flexible-link planar mechanism by means of a linearized model in the state-space form for design of a vibration controller," *Journal of Sound and vibration*, vol. 240, no. 2, pp. 241–262, 2001.

[20] B. Anderson, J. Moore, and D. Naidu, *Optimal control: linear quadratic methods*. Prentice Hall Englewood Cliffs, NJ, 1990.